

Tropical cyclone genesis

J. H. Koh and
C. M. Brierley

Tropical cyclone genesis across palaeoclimates

J. H. Koh and C. M. Brierley

Department of Geography, University College London, London WC1E 6BT, UK

Received: 10 December 2014 – Accepted: 12 January 2015 – Published: 6 February 2015

Correspondence to: C. M. Brierley (c.brierley@ucl.ac.uk)

Published by Copernicus Publications on behalf of the European Geosciences Union.

Title Page

Abstract

Introduction

Conclusions

References

Tables

Figures



Back

Close

Full Screen / Esc

Printer-friendly Version

Interactive Discussion



Abstract

Tropical cyclone genesis is investigated for the Pliocene, Last Glacial Maximum (LGM) and the mid-Holocene through analysis of five climate models. The genesis potential index is used to estimate this from large scale atmospheric properties. The mid-Pliocene and LGM characterise periods where carbon dioxide levels were higher and lower than pre-industrial respectively, while the mid-Holocene differed primarily in its orbital configuration. The number of tropical cyclones formed each year is found to be fairly consistent across the various palaeoclimates. Although there is some model uncertainty in the change of global annual tropical cyclone frequency, there are coherent changes in the spatial patterns of tropical cyclogenesis.

During the Pliocene and LGM, changes in carbon dioxide led to sea surface temperature changes throughout the tropics, yet the potential intensity of tropical cyclones appears relatively insensitive to these variations. Changes in tropical cyclone genesis during the mid-Holocene are observed to be asymmetric about the Equator: genesis is reduced in the Northern Hemisphere, but enhanced in the Southern Hemisphere. This is clearly driven by the altered seasonal insolation. Nonetheless, the enhanced seasonality may have driven localised effects on tropical cyclone genesis, through changes to the strength of monsoons and shifting of the inter-tropical convergence zone. Trends in future tropical cyclone genesis are neither consistent between the five models studied, nor with the palaeoclimate results. It is not clear why this should be the case.

1 Introduction

Tropical cyclones (TC) constitute one of the most powerful forces of nature and can cause severe destruction to human life and property. How TC genesis may change in the face of climate change is thus an area of strong interest. Past studies using high resolution general circulation models (GCMs) have generally suggested that cyclone intensity would strengthen, yet cyclone genesis would decline in a warming climate

CPD

11, 181–220, 2015

Tropical cyclone genesis

J. H. Koh and
C. M. Brierley

Title Page

Abstract

Introduction

Conclusions

References

Tables

Figures



Back

Close

Full Screen / Esc

Printer-friendly Version

Interactive Discussion



Tropical cyclone genesis

J. H. Koh and
C. M. Brierley

Title Page

Abstract

Introduction

Conclusions

References

Tables

Figures



Back

Close

Full Screen / Esc

Printer-friendly Version

Interactive Discussion



(Knutson et al., 2010). However, recent analyses of future simulations performed as part of the Coupled Model Intercomparison Project Phase 5 (CMIP5) appear equivocal: statistical downscaling indicates an increase in both cyclone intensity and genesis (Emanuel, 2013); dynamical downscaling indicates an increase in intensity combined with a reduction in frequency (Knutson et al., 2013); tracking algorithms of global coupled models do likewise (Camargo, 2013); large-scale cyclogenesis indices have shown both frequency increases (Emanuel, 2013) and decreases (Camargo, 2013).

Understanding past climates provides a means for scientists to contextualise future climate change impacts. Palaeoclimates with altered climate forcings, such as the elevated levels of carbon dioxide during the Pliocene period, may provide clues about how the trend of cyclone genesis would respond to ongoing anthropogenic emissions of greenhouse gases.

The mid-Piacenzian warm portion of the mid-Pliocene (around 3 million years ago, henceforth “Pliocene”) was a recent episode in Earth’s geological history where mean global temperatures were warmer by 2–3°C compared to modern times (Haywood et al., 2013), but the warming was not constant across the globe. Sea surface temperatures (SST) anomalies were more pronounced at the higher latitudes (up to 20°C in the high Arctic; Ballantyne et al., 2009), while the lower latitudes exhibited minimal change in places (Dowsett et al., 2010). The geography of the continents and oceans were relatively similar to earth’s current configuration (Haywood et al., 2011). Carbon dioxide concentrations were at or near present day levels during the mid-Pliocene (Pagani et al., 2009). There is potential for using the Pliocene to learn about the equilibrium state of the earth’s warm climate following anthropogenic greenhouse gas influence (Haywood et al., 2009).

Meanwhile, the icehouse climate of the Last Glacial Maximum (LGM) at 21ka serves as a contrast to the current greenhouse climate. Proxy estimates by Annan and Hargreaves (2013) suggest that LGM tropical SST was around 1.6°C lower than pre-industrial, while global surface air temperatures were 3.1–4.7°C cooler. Given the relatively similar orbital parameters controlling Earth’s solar insolation during the Pliocene,

LGM and pre-industrial intervals, the Palaeoclimate Model Intercomparison Project (PMIP)'s focus on these times help facilitate studies that examine the effect of carbon dioxide concentration changes on the tropical climate (Table 1).

On the other hand, simulations for the mid-Holocene at 6ka differ from pre-industrial conditions mainly in the orbital parameters that result in an increased insolation in the high latitudes. The tropical region during the mid-Holocene interval might have encountered slightly elevated sea-surface temperatures (SST) of around 1 °C (Gagan et al., 1998), although recent studies indicate some uncertainty in terms of negative SST anomaly for regions such as the western Indian Ocean (Kuhnert et al., 2014). Despite the limited proxy record agreement on whether tropical oceans may have warmed (Koutavas et al., 2002; Rambu et al., 2004; Stott et al., 2004), prior PMIP simulations suggest SST in the Northern Hemisphere was generally warmer by less than 1 °C in the mid-Holocene period compared to the pre-industrial era, and the Southern Hemisphere might have been slightly cooler (Braconnot et al., 2007).

Given the lack of data on tropical cyclone frequency for these palaeoclimates, model simulation studies do not seek to verify model response on cyclone formation, but rather aim to describe tropical cyclone trends with the assumption that signals would be detectable by using indicators such as cyclogenesis potential. Using PMIP Phase 2 (PMIP2) data, studies have been conducted to investigate TC genesis activity during the LGM and mid-Holocene intervals. For the LGM, Korty et al. (2012a) observed higher annual cyclone genesis relative to the pre-industrial era. For the mid-Holocene interval, Korty et al. (2012b) demonstrated that the difference in distribution of the top-of-atmosphere (TOA) radiation in comparison to the pre-industrial control altered the seasonal cycle of potential intensity in the Northern Hemisphere. There was mixed response in TC genesis for the mid-Holocene relative to the pre-industrial period, with slightly lower TC activity in the Northern Hemisphere (and slightly higher in the Southern Hemisphere).

This study aims to investigate whether similar behaviours are seen in the subsequent generation of PMIP; namely the PMIP3 model ensemble. The related Pliocene

Tropical cyclone genesis

J. H. Koh and
C. M. Brierley

[Title Page](#)[Abstract](#)[Introduction](#)[Conclusions](#)[References](#)[Tables](#)[Figures](#)[Back](#)[Close](#)[Full Screen / Esc](#)[Printer-friendly Version](#)[Interactive Discussion](#)

8.5) is likewise analysed as an example future elevated carbon dioxide concentration scenario. The GCMs that have been included for this study are outlined in Table 2.

In situations where a pre-computed monthly climatology of a particular simulation is not available on the Earth System Federation Grid, a 50 year time-slice from the end of the interval of interest is used to generate the monthly climatology data so as to minimise stochastic effects, model drift and internal variability. To estimate the ranges associated with internal variability, ten decadal time-slices are taken from a hundred year dataset of the pre-industrial dataset of each model. The standard deviation (SD) is found to be within 1–3% of the pre-industrial (PI) TC genesis annual frequencies simulated across the five GCMs (Table 2).

3 Genesis potential index

The use of a metric related to genesis potential is particularly useful to describe cyclogenesis as the grid resolution of most GCMs is not sufficiently refined to simulate mesoscale processes taking place in TCs. Many studies have used genesis potential indices as a less computationally intensive approach to describe TC genesis (Bruyère et al., 2012; Camargo et al., 2007; Emanuel and Nolan, 2004; Korty et al., 2012a, b; Menkes et al., 2012; Tippett et al., 2010).

Gray (1975) pioneered work on the genesis potential index (GPI) by demonstrating the use of selected diagnostics such as mid-troposphere humidity, vertical shear of the horizontal winds between the high and low level troposphere, low level relative vorticity, and thermal parameters related to SST to characterise climatic conditions that are favourable for cyclone genesis. The subsequent GPI improved by Emanuel and Nolan (2004) is considered state-of-the-art (Tippett et al., 2010) and incorporates the potential intensity theory (Emanuel, 1988; Holland, 1997) that evaluates the maximum wind speed that may be attainable using the available thermodynamic energy imparted from the atmospheric environment and the sea surface to the cyclone.

Tropical cyclone genesis

J. H. Koh and
C. M. Brierley

[Title Page](#)

[Abstract](#)

[Introduction](#)

[Conclusions](#)

[References](#)

[Tables](#)

[Figures](#)



[Back](#)

[Close](#)

[Full Screen / Esc](#)

[Printer-friendly Version](#)

[Interactive Discussion](#)



The GPI proposed by Emanuel and Nolan (2004) serves to synergise the thermodynamic and kinematic factors affecting TC genesis into a single index. With the aim of facilitating comparison with previous investigations into palaeoclimate cyclone genesis, the “clipped vorticity” version of the GPI employed by Korty et al. (2012a, b) has likewise been adopted for this study:

$$\text{GPI} = \frac{b[\min(|\eta|, 4 \times 10^{-5})]^3 [\max(\text{PI} - 35, 0)]^2}{\chi_m^{\frac{4}{3}} [25 + V_{\text{shear}}]^4} \quad (1)$$

Here, η represents the absolute vorticity computed at the 850 hPa level (Nolan and Rappin, 2008), V_{shear} is the 200–850 hPa wind shear value, χ_m is the moist entropy deficit. PI is the maximum potential intensity a TC can theoretically achieve (a potential intensity of less than 35 ms^{-1} would not be classified as a tropical storm). Due to the inherent biases in convection schemes and parameterisations employed by GCMs, the global annual total TC genesis has to be calibrated (Emanuel et al., 2008b). b is therefore an empirically derived normalisation factor that calibrates the GPI to achieve a pre-industrial control annual cyclone genesis frequencies on the order of the roughly eighty storms observed per year in the modern period. Following Korty et al. (2012a, b), a value of 5.55×10^{-5} is used throughout for the value of b .

Wind shear and absolute vorticity are the two kinematic factors of the GPI, while potential intensity and moist entropy deficit are both thermodynamic factors (Korty et al., 2012a). Wind shear, which is the vertical shear of the horizontal winds between the upper and lower troposphere, causes asymmetries in the developing cyclone which results in the ventilation of the upper level warm core through the flushing of relatively cooler and drier air from the top (Frank and Ritchie, 2001). Stronger wind shear therefore influences inflow dynamics and weakens cyclone formation (Riemer et al., 2013). While noting caveats where such two-level vector differentials may be inadequate to describe the resultant wind shear in some scenarios (Velden and Sears, 2014), this

**Tropical cyclone
genesis**

J. H. Koh and
C. M. Brierley

Title Page

Abstract

Introduction

Conclusions

References

Tables

Figures



Back

Close

Full Screen / Esc

Printer-friendly Version

Interactive Discussion



study defines the wind shear as the difference between the 200 and 850 hPa winds given its ease of computation.

Meanwhile, the vorticity serves as a spin-up mechanism that initiates cyclone formation in a recirculating flow that is quasi-closed in the lower troposphere. Taking the analogy of a protective pouch, the quasi-closed streamlines surround the enhanced vorticity while nurturing the thermodynamic and convective processes that favour TC development (Tory et al., 2012). Tippett et al. (2010) observed that vorticity has a greater influence on cyclone formation at lower latitudes, and other factors play a greater role at higher latitudes. Kerty et al. (2012a, b) subsequently incorporated a “clipped vorticity” diagnosis in place of absolute vorticity in the GPI, so as to moderate its response in over-estimating TC activity for the sub-tropics. Potentially, the clipping threshold may have varied in the past through large-scale changes in the atmosphere circulation. The sensitivity of different clipping thresholds was investigated in the case of the Pliocene period using the MIROC model. Changes in the clipping threshold appear to have little substantive impact on the resulting change in GPI for this study.

The non-dimensional term (χ_m) measures the moist entropy difference between the mid-troposphere and the boundary layer that is derived from asymmetric cyclone models (Emanuel, 1995b), as shown below:

$$\chi_m = \frac{s_b - s_m}{s_o^* - s_b} \equiv \frac{s^* - s_m}{s_o^* - s_b} \quad (2)$$

s_m , s_b and s_o^* represent the moist entropies of the mid-troposphere layer, boundary layer, and the sea surface saturation entropy respectively. Taking the assumption that the lapse rate of the tropical atmosphere is largely moist adiabatic (Emanuel et al., 2008b), s^* which is the saturation entropy above the boundary layer, is assumed to be constant throughout the atmospheric column. This allows the numerator term in Eq. (2) to be evaluated at 600 hPa which is taken to represent the mid-troposphere as defined by Emanuel (1994). s_b and s_o^* are calculated at 925 hPa for the boundary layer and at the sea surface respectively. Physically, a larger χ_m signifies a longer duration

Tropical cyclone genesis

J. H. Koh and
C. M. Brierley

[Title Page](#)[Abstract](#)[Introduction](#)[Conclusions](#)[References](#)[Tables](#)[Figures](#)[Back](#)[Close](#)[Full Screen / Esc](#)[Printer-friendly Version](#)[Interactive Discussion](#)

needed for an initial perturbation to moisten the middle troposphere before intensification occurs (Emanuel et al., 2008b).

Taking on the analogy of a cyclone's evolution process as equivalent to Nature's Carnot engine (Emanuel, 1988, 1991), the potential intensity diagnostic derived by Bister and Emanuel (1998, 2002) that takes into account the effects of dissipative heating is:

$$\text{Potential Intensity (PI)} = \sqrt{\frac{C_k}{C_d} \frac{\text{SST}}{T_o} (\text{CAPE}^* - \text{CAPE}_b)} \quad (3)$$

C_k and C_d are the surface exchange coefficients for enthalpy and momentum. Its ratio could range between 0.1 to 1.3 (Montgomery et al., 2010) and is likely between 0.75 and 1.5 for naturally occurring cyclones (Emanuel, 1995a). In this study, a ratio of $C_k/C_d = 1$ is taken to allow for ease of comparison with previous work that used a similar assumption (Korty et al., 2012a). T_o is an entropy-weighted mean temperature of the outflow. The convective available potential energy (CAPE^*) describes an air parcel of maximum wind intensity that has been earlier saturated at the sea surface, while CAPE_b describes a boundary layer air parcel which has been isothermally lowered from an equivalent air parcel of maximum wind intensity. Climate variables that are required for the potential intensity calculation include SST and pressure of the sea surface, as well as the humidity and temperature profile of the atmospheric column. The calculation of potential intensity for this study is facilitated by the use of an previously applied algorithm (Emanuel et al., 2008a).

Tropical cyclone genesis

J. H. Koh and
C. M. Brierley

[Title Page](#)[Abstract](#)[Introduction](#)[Conclusions](#)[References](#)[Tables](#)[Figures](#)[Back](#)[Close](#)[Full Screen / Esc](#)[Printer-friendly Version](#)[Interactive Discussion](#)

4 Results

4.1 Potential intensity

In the tropical region, the Pliocene saw higher SSTs by about 2 °C relative to the pre-industrial control (and the mid-Holocene), while SSTs were lower by about 2 °C at the LGM (Fig. 1). Korty et al. (2012a) suggested that high values of potential intensity, typically higher than 55 ms⁻¹, are needed to induce deep tropospheric convection in TC genesis. Interestingly the locations of the 55 ms⁻¹ potential intensity contour appears to be relatively insensitive to these wholesale SST changes. For example, the contour in the North Pacific is associated with SSTs ranging from 26 °C during the Pliocene to 22 °C at the LGM.

During the Pliocene, there is a reduction in potential intensity over the North Atlantic, despite an SST increase in the same region (Fig. 1b). This supports research showing that absolute SST by itself can be an inadequate indicator of storm strength (Vecchi et al., 2008). Whilst, this may appear to depart from early understanding of threshold SST values (e.g. 26 °C) in influencing cyclone genesis (Palmen, 1948), it rather underscores the importance of other factors, such as atmospheric humidity and upper troposphere outflow temperature relative to the SST, that jointly determine the magnitude of energy available to a tropical cyclone (Emanuel, 1998).

4.2 Pre-industrial

The pre-industrial serves as a useful reference climate as it is before Earth's environment came under substantial anthropogenic influence, especially over the tropical oceans (Lewis and Maslin, 2014). Figure 2 illustrates the genesis potential simulated from the various GCMs in their pre-industrial simulations. The Northern Hemisphere shows cyclone genesis potential for the peak storm periods of July, August, September and October (JASO), while the Southern Hemisphere corresponds to the peak storm

CPD

11, 181–220, 2015

Tropical cyclone genesis

J. H. Koh and
C. M. Brierley

Title Page

Abstract

Introduction

Conclusions

References

Tables

Figures



Back

Close

Full Screen / Esc

Printer-friendly Version

Interactive Discussion



period of January, February, March, April (JFMA). Monthly storm genesis will be discussed in Sect. 4.6.

The GPI distribution of the various GCMs compares favourably with the outcomes from similar model analysis by Camargo (2013) for the pre-industrial period, despite the use of different genesis indices. All models simulate cyclone genesis in the eastern and western Pacific in the Northern Hemisphere during JASO, as well as the eastern Pacific near the South Pacific Convergence Zone (SPCZ) during JFMA. Stronger cyclone genesis in the southern Indian Ocean is found during JFMA, with limited genesis in the northern Indian Ocean during JASO apart from some areas such as the northern Bay of Bengal. The North Atlantic features some genesis potential at the deep and sub-tropics, but the South Atlantic shows almost negligible potential for TC genesis. These features are all shown in observations of tropical cyclone genesis (Knapp et al., 2010).

However the various models do show some biases. CCSM4, HadCM3 and IPSL-CM5A-LR exhibit greater intensity of cyclone genesis over the North Pacific and at the SPCZ; as compared to FGOALS-G2 and MIROC-ESM which appear to have a more extensive area of cyclone genesis but with lower intensity. While IPSL-CM5A-LR suggests that the central-western Pacific would experience the greatest intensity of cyclone genesis, CCSM4 and HadCM3 show the greatest genesis intensity arising in the north-eastern Pacific. MIROC-ESM simulates its strongest genesis intensity in the maritime continent region. FGOALS-G2 shows a relatively uniform strength of genesis potential across all the oceans, apart from an area of increased intensity in the eastern North Pacific and Philippine Sea. The genesis potential also stretches across a greater area in FGOALS-G2 relative to the other models.

The ensemble mean (Fig. 2f) is obtained by interpolating the individual model GPI onto the HadCM3 grid which is comparatively lower in resolution. The ensemble also reveals highly similar distribution of genesis intensity for regions such as the North Atlantic, Pacific and Indian oceans in comparison with the 0 ka genesis potential from Korty et al. (2012a) simulated using PMIP2 data from seven GCMs. In both instances,

CPD

11, 181–220, 2015

Tropical cyclone genesis

J. H. Koh and
C. M. Brierley

Title Page

Abstract

Introduction

Conclusions

References

Tables

Figures



Back

Close

Full Screen / Esc

Printer-friendly Version

Interactive Discussion



the highest intensity of genesis potential is located between the 10–20° latitude belts of the respective peak storm periods of both hemispheres, and both are of comparable cumulative genesis magnitude of between 3–5 occurrences $\text{m}^{-2}\text{month}^{-1}$ (not shown). The pre-industrial climate thus exhibits consistency in cyclogenesis between the PMIP3 and PMIP2 simulations (only HadCM3 occurs in both ensembles).

4.3 Mid-Holocene

The key difference between the mid-Holocene and pre-industrial climate lies in the changes in solar insolation arising from different angular precession (Table 1). As a result, the Northern Hemisphere receives proportionally greater insolation during its storm season compared to the Southern Hemisphere. The summer and annual mean insolation for the high latitudes in both hemispheres is also increased (Braconnot et al., 2007).

These insolation changes drive responses in diagnosed cyclogenesis across the five models (Fig. 3). CCSM4 shows the strongest response while the response from MIROC is relatively muted. HadCM3 exhibits a reduction of genesis potential in the Northern Hemisphere compensated for by an increase in the Southern Hemisphere. The response of FGOALS and CCSM bear similarities to each other in that their bands of TC genesis in the North Pacific become more zonal. IPSL and MIROC show little change from the pre-industrial.

The ensemble genesis potential for the mid-Holocene (Fig. 4a) shares largely similar distribution as the pre-industrial period (Fig. 2), although some localised differences in genesis strength are observed (Fig. 4b). The Southern Hemisphere exhibits a weak change from mid-Holocene over pre-industrial, except for pockets around Northern Australia that show a stronger increase in genesis magnitude. Magnitude changes are more salient in the Northern Hemisphere. A slight decrease in genesis potential is seen in the North Atlantic. Changes in the North Pacific occur with dipole patterns at the periphery of the East and West Pacific indicating shifts in the location of cyclone genesis.

Tropical cyclone genesis

J. H. Koh and
C. M. Brierley

Title Page

Abstract

Introduction

Conclusions

References

Tables

Figures



Back

Close

Full Screen / Esc

Printer-friendly Version

Interactive Discussion



**Tropical cyclone
genesis**J. H. Koh and
C. M. Brierley[Title Page](#)[Abstract](#)[Introduction](#)[Conclusions](#)[References](#)[Tables](#)[Figures](#)[Back](#)[Close](#)[Full Screen / Esc](#)[Printer-friendly Version](#)[Interactive Discussion](#)

There is a good agreement across the ensemble on the sign of the mid-Holocene change in most areas amongst the five GCMs (Fig. 4c). There is a general decrease in cyclone genesis in the Northern Hemisphere, and an increase in cyclone genesis as one moves polewards in the Southern Hemisphere. Although several regions show strong agreement in increased cyclone genesis, such as the South Pacific and South Atlantic, the fact that the increased cyclone genesis are not depicted in Fig. 4b indicates only a very small degree of cyclone genesis increase in these areas.

The results for the mid-Holocene using these PMIP3 models compare well with findings from Korty et al. (2012b) that detail cyclone genesis using an ensemble from ten GCMs from PMIP2. The magnitude and distribution of genesis potential share similar patterns across all oceans. Nonetheless this study simulates a slightly weaker genesis potential for the western South Indian Ocean and the South Atlantic, as well as a slightly weaker increase in genesis potential for mid-Holocene over pre-industrial in both hemispheres. The model agreement (Fig. 4c) shares remarkable similarity with Korty et al. (2012b) on the sign of change in genesis potential of the mid-Holocene era compared to the pre-industrial period, where the Northern Hemisphere shows a decrease in genesis potential while the Southern Hemisphere shows general increase in genesis potential, especially in the higher tropical latitudes.

4.4 Last Glacial Maximum (LGM)

During the LGM, the tropics experienced cooling of -5 to -2°C over land, while most of the tropical surface ocean did not encounter cooling beyond -2°C especially in the Southern Hemisphere (Waelbrook et al., 2009). The LGM mean tropical SST from the five GCMs in this study during the peak storm period is 2.0°C cooler than pre-industrial. Simulated genesis potential responses for the LGM appear mixed (Fig. 5). CCSM, HadCM3 and MIROC show generally stronger genesis, while FGOALS and IPSL show a weakening in genesis potential relative to pre-industrial. All of the models show some form of compensation, indicative of shifts in the relative dominance of the TC formation locales.

Tropical cyclone genesis

J. H. Koh and
C. M. Brierley

Title Page

Abstract

Introduction

Conclusions

References

Tables

Figures



Back

Close

Full Screen / Esc

Printer-friendly Version

Interactive Discussion



The key areas of Pliocene cyclone genesis in the ensemble mean can be found in the eastern and western areas of the North Pacific, the SPCZ and central region of the South Pacific, as well as the north-western corner of the South Indian Ocean (Fig. 8a). In terms of the difference in genesis potential between the Pliocene and pre-industrial periods (Fig. 8b), the North Atlantic, North Pacific, and South Indian oceans and the SPCZ region would largely experience a decline in genesis during the Pliocene. Nonetheless, there may be localised areas where genesis potential could have increased, such as to the east of New Guinea in the South Pacific.

This large-scale pattern appears to be robust as most models suggest a general decrease in genesis potential for the Pliocene relative to the pre-industrial for most oceans (Fig. 8c), although the magnitude of change might be small in areas such as the South Atlantic and eastern South Pacific. There appears to be weaker model agreement on the sign of change for the subtropical latitudes for the Pacific and Indian oceans in both hemispheres, although a slight increase in genesis potential may be expected.

4.6 Genesis frequency

Figure 9 illustrates the annual TC genesis frequency generated from the five GCMs across the various palaeoclimates as a percentage of the pre-industrial. The ensemble-mean annual genesis frequency for the Pliocene, LGM and mid-Holocene are determined to be 91, 97 and 100 % of the pre-industrial respectively.

Estimating the natural variability of an ensemble mean number is problematic. As a conservative measure, we take that from the model with the highest internal variability (HadCM3) that has a SD (σ) of 2.9%. Given that the ensemble annual frequencies are generally within the standard measure of 2σ (Haywood et al., 2013), the annual genesis frequencies for both the LGM and mid-Holocene is considered to have not deviated significantly from the pre-industrial era. Whilst the ensemble mean value for the Pliocene is statistically significant by this metric, in fact the magnitude of the reduction is driven solely by the HadCM3 member (the ensemble average without it is 100 % of

the pre-industrial). The assumption of a Gaussian distribution inherent in this metric of significance is clearly not valid for this ensemble. It is therefore not clear we can consider the reduction seen in Pliocene ensemble as robust feature.

In Fig. 10, the Northern (Southern) Hemisphere peak in JASO (JFMA) appears consistent across the various intervals, justifying this study's choice of the peak storm seasons for the respective hemisphere. Previous work from Korty et al. (2012a, b) using PMIP2 data showed a stronger peak from the Southern Hemisphere relative to the north, while this study suggests a stronger Northern Hemisphere peak. This suggests that the PMIP3 simulations may have improved accuracy in describing present day trends of a more conducive Northern Hemisphere for cyclone genesis (Gray, 1968; Klotzbach, 2006; Webster et al., 2005).

The observation of a slight increase in LGM cyclone genesis relative to the pre-industrial period is consistent with earlier work by Korty et al. (2012a). The reduced TC genesis associated with the warm Pliocene conforms to the Knutson et al. (2010) view of future behaviour. It does differ from the sole prior Pliocene TC study (Fedorov et al., 2010). However that work, aimed at the early Pliocene and using a statistical downscaling approach, involved the imposition of a substantially different SST field.

For the mid-Holocene epoch, a salient increase in October activity is observed by Korty et al. (2012b), which has been attributed to a delayed SST response from the TOA insolation forcing, resulting in a shift of the Northern Hemisphere storm season. However, this trend is not observed in this study. Annual SST changes are found to have varied minimally relative to the pre-industrial (Fig. 1), suggesting that the ocean component during the mid-Holocene may play a lesser role in comparison to the Pliocene and LGM epochs where more substantial SST changes are observed.

5 Discussion

During the Pliocene and LGM, changes in carbon dioxide lead to sea surface temperature (SST) changes throughout the tropics, yet the potential intensity of TCs are

CPD

11, 181–220, 2015

Tropical cyclone genesis

J. H. Koh and
C. M. Brierley

Title Page

Abstract

Introduction

Conclusions

References

Tables

Figures



Back

Close

Full Screen / Esc

Printer-friendly Version

Interactive Discussion



along with slight reduction in the Northern Hemisphere (Fig. 4c). This is associated with higher entropy deficit in the Northern Hemisphere hindering cyclone genesis compared to the Southern Hemisphere (not shown). The potential intensity increases slightly at all latitudes.

5.1 Relationship to future projections

Records do not currently exist to either confirm or refute the tropical cyclogenesis changes simulated by this ensemble. They probably never will. Yet the Earth will shortly experience carbon dioxide concentrations beyond those of the Pliocene period. Therefore, it is interesting to consider how the results above correspond to future projections of tropical cyclogenesis. One further motivation to do this is that the palaeoclimate simulations are all equilibrium experiments, whilst the future projections are transient. It is therefore anticipated that the climate change signal will be easier to detect in the palaeoclimate simulations. In transient simulations, large-scale forcings may not fully account for the observed variability (Menkes et al., 2012), as stochastic effects may potentially account for up to half of the observed variability (Jourdain et al., 2010).

The RCP8.5 scenario is used to project how TC genesis may develop in future. It is chosen as it is the most extreme scenario and so should have the biggest signal. In this scenario, carbon dioxide concentrations reach 936 ppmv by 2100 (Collins et al., 2013), more than double the level in the Pliocene simulations.

The GCMs selected in this study all show future changes in TC genesis (as calculated by the GPI) under the RCP8.5 transient scenario (Fig. 11). Yet these trends are not consistent between the models. Note that HadCM3 has not contributed results for RCP8.5, so a later generation of the model (HadGEM2) has been substituted. Two models suggest an increase in TC genesis, while three models suggest a decrease, resulting in an ensemble mean with a trend of slightly reduced TC genesis by 2095. The future response is also seemingly inconsistent with the palaeoclimate responses in the same GCM. For example, MIROC shows a decrease in cyclone activity in the

Tropical cyclone genesis

J. H. Koh and
C. M. Brierley

Title Page

Abstract

Introduction

Conclusions

References

Tables

Figures



Back

Close

Full Screen / Esc

Printer-friendly Version

Interactive Discussion



warm Pliocene and an increase during the LGM: counter-intuitively it also shows an increase under RCP8.5.

Interestingly, the multi-model mean GPI difference between the future RCP8.5 (2071–2100) scenario and historical (1971–2000) simulation from Camargo (2013) shows an opposite response to the difference for the equilibrium Pliocene-control difference in Fig. 8b of this study. The transient RCP8.5 GPI difference in Camargo (2013) suggests a global increase, except for a small area in the central South Pacific where a decrease is expected. Meanwhile the equilibrium Pliocene-pre-industrial difference in this study shows a general decrease, and a small region of the western South Pacific has an increase in GPI. The stark difference in cyclogenesis trends between the RCP8.5 and Pliocene therefore throws some questions on the suitability for the choice of the Pliocene as a projection of modern day greenhouse climate, at least in terms of cyclogenesis projections.

Emanuel (2013) downscaled six CMIP5 GCMs for the RCP8.5 projection, and concluded that an increase in future global tropical cyclone activity might be expected. The same paper also acknowledged that other modelling groups obtained contrasting results where modest decreases (Knutson et al., 2010) and no robust change (Camargo, 2013) in future tropical cyclone activity had been detected. Two models (CCSM4 and HADGEM2-ES) that Emanuel (2013) used for his RCP8.5 scenario conclusions are also incorporated in this study, but an increasing trend is not detected for the two particular models. Potential reasons that could account for the difference include the use of a modified “clipped” vorticity GPI in this study, and a different choice of 250–850 hPa tropospheric wind shear in Emanuel (2013). The striking difference in TC activity outcomes, despite a similar GCM choice, suggests that the GPI may be highly sensitive to adjustments in diagnostic definition.

Kossin et al. (2014) showed that the lifetime-maximum intensity of tropical cyclones is migrating polewards at a rate of about one degree of latitude per decade, similar to the rate of expansion of the tropics (Lucas et al., 2014). No coherent message about poleward expansion of TC genesis was found in this ensemble and changes in TC

CPD

11, 181–220, 2015

Tropical cyclone genesis

J. H. Koh and
C. M. Brierley

Title Page

Abstract

Introduction

Conclusions

References

Tables

Figures



Back

Close

Full Screen / Esc

Printer-friendly Version

Interactive Discussion



genesis are found largely in the 10–20° regions of both hemispheres, with minimum adjustment in the sub-tropics.

6 Conclusions

The global frequency of tropical cyclone formation is estimated to have been relatively constant over the range of past climates using a genesis potential index (GPI). This range encompasses both greenhouse (Pliocene) and icehouse (Last Glacial Maximum) climates and changing orbital forcing. These conditions are thought to represent the extremes of climates Earth has experienced in the past three million years. At times the spread of model estimates of the global, total number of tropical cyclones can be large (Fig. 9), something that is especially noticeable for the Pliocene simulations.

The ensemble shows much higher levels of consistency on the regional scale. All five models agree on a reduction in the genesis of the North Atlantic hurricanes at the Last Glacial Maximum; compensated for by an increase in potential cyclogenesis in the central North Pacific, to a greater or lesser degree. Presumably this is a circulation response to the existence of a large ice-sheet over North America. A qualitatively similar feature has been seen previously (Korty et al., 2012a), but would obviously not be expected in the reverse in future projections. The mid-Holocene ensemble shows alterations of GPI associated with shifts in the intertropical convergence zone driven by the altered incoming solar distribution. Again the results from this ensemble are qualitatively similar to those from prior model ensembles (Korty et al., 2012b).

The tropical cyclone distribution for the mid-Pliocene has not previously been considered. Fedorov et al. (2010) anticipated an expansion of cyclone location, strength and magnitude in response to the observed weakened tropical temperature gradients of the early Pliocene (Brierley et al., 2009). The PlioMIP ensemble of the mid-Pliocene does not show those weakened gradients (Haywood et al., 2013; Brierley, 2014) nor their associated TC genesis pattern. Rather there are large swathes of the ocean that show a robust reduction in genesis potential index.

Tropical cyclone genesis

J. H. Koh and
C. M. Brierley

Title Page

Abstract

Introduction

Conclusions

References

Tables

Figures



Back

Close

Full Screen / Esc

Printer-friendly Version

Interactive Discussion



Tropical cyclone genesis

J. H. Koh and
C. M. Brierley

Title Page

Abstract

Introduction

Conclusions

References

Tables

Figures



Back

Close

Full Screen / Esc

Printer-friendly Version

Interactive Discussion



One motivation for studying the past climate tropical cyclone response is to investigate its relationship to future projections. The genesis potential under the RCP8.5 scenario was computed and contrasted with the palaeoclimate response. There is no simple relationship that emerges between global tropical cyclogenesis and say CO₂ level or hemispheric temperature. This result means that analysis of the changes in total frequency of tropical cyclone remains much less robust than the changes in the regional response noted above. The conclusion is further strengthened by the apparent sensitivity of projected future global frequency to the precise genesis potential index used – with our analysis not fully supporting either the results of Emanuel (2013) nor the opposing results of Camargo (2013) despite all three using the same simulations.

Acknowledgements. The work was made possible through a scholarship awarded to J.H. Koh from the Ministry of the Environment and Water Resources, Singapore. The authors thank Suzana J. Camargo for her useful comments on GPI metrics and Kerry Emanuel for his assistance, not least his release of the Potential Intensity matlab routine. The assistance of Fran Bragg, Camille Contoux, Wing-Le Chan and Weipeng Zheng was essential to procure the necessary Pliocene simulation files. The creation of monthly climatologies for the PMIP3 simulations by Jean-Yves Peterschmitt was particularly helpful.

References

- Annan, J. D. and Hargreaves, J. C.: A new global reconstruction of temperature changes at the Last Glacial Maximum, *Clim. Past*, 9, 367–376, doi:10.5194/cp-9-367-2013, 2013.
- Bister, M. and Emanuel, K. A.: Dissipative heating and hurricane intensity, *Meteorol. Atmos. Phys.*, 65, 233–240, 1998.
- Bister, M. and Emanuel, K. A.: Low frequency variability of tropical cyclone potential intensity 1. Interannual to interdecadal variability, *J. Geophys. Res.*, 107, 4801, 2002.
- Braconnot, P., Otto-Bliesner, B., Harrison, S., Joussaume, S., Peterchmitt, J.-Y., Abe-Ouchi, A., Crucifix, M., Driesschaert, E., Fichet, Th., Hewitt, C. D., Kageyama, M., Kitoh, A., Laîné, A., Loutre, M.-F., Marti, O., Merkel, U., Ramstein, G., Valdes, P., Weber, S. L., Yu, Y., and Zhao, Y.: Results of PMIP2 coupled simulations of the Mid-Holocene and Last Glacial Maxi-

Tropical cyclone genesis

J. H. Koh and
C. M. Brierley

Title Page

Abstract

Introduction

Conclusions

References

Tables

Figures



Back

Close

Full Screen / Esc

Printer-friendly Version

Interactive Discussion



mum – Part 1: experiments and large-scale features, *Clim. Past*, 3, 261–277, doi:10.5194/cp-3-261-2007, 2007.

Braconnot, P., Luan, Y., Brewer, S., and Zheng, W.: Impact of Earth's orbit and freshwater fluxes on Holocene climate mean seasonal cycle and ENSO characteristics, *Clim. Dynam.*, 38, 1081–1092, 2012.

Brierley, C. M.: Interannual climate variability seen in the Pliocene Model Intercomparison Project, *Clim. Past Discuss.*, 10, 3787–3820, doi:10.5194/cpd-10-3787-2014, 2014.

Bruyère, C. L., Holland, G. J., and Towler, E.: Investigating the use of a genesis potential index for tropical cyclones in the North Atlantic Basin, *J. Climate*, 25, 8611–8626, 2012.

Camargo, S. J.: Global and regional aspects of tropical cyclone activity in the CMIP5 models, *J. Climate*, 26, 9880–9902, 2013.

Camargo, S. J., Sobel, A. H., Barnston, A. G., and Emanuel, K. A.: Tropical cyclone genesis potential index in climate models, *Tellus A*, 59, 428–443, 2007.

Camargo, S. J., Ting, M., and Kushnir, Y.: Influence of local and remote SST on North Atlantic tropical cyclone potential intensity, *Clim. Dynam.*, 40, 1515–1529, 2013.

Chan, W.-L., Abe-Ouchi, A., and Ohgaito, R.: Simulating the mid-Pliocene climate with the MIROC general circulation model: experimental design and initial results, *Geosci. Model Dev.*, 4, 1035–1049, doi:10.5194/gmd-4-1035-2011, 2011.

Collins, M., Knutti, R., Arblaster, J. M., Dufresne, J.-L., Fichefet, T., Friedlingstein, P., Gao, X., Gutowski, W. J., Johns, T. C., Krinner, G., Shongwe, M., Tebaldi, C., Weaver, A. J. and Wehner, M. F.: Long-term climate change: projections, commitments and irreversibility, in: Stocker, T. F., Qin, D., Plattner, G.-K., Tignor, M., Allen, S. K., Boschung, J., Nauels, A., Yu, X., Bex, V. and Midgely, P. M., *Climate Change 2013: The Physical Science Basis*, Cambridge University Press, Cambridge, UK and New York, NY, USA, 1029–1136, 2013.

Collins, W. J., Bellouin, N., Doutriaux-Boucher, M., Gedney, N., Halloran, P., Hinton, T., Hughes, J., Jones, C. D., Joshi, M., Liddicoat, S., Martin, G., O'Connor, F., Rae, J., Senior, C., Sitch, S., Totterdell, I., Wiltshire, A., and Woodward, S.: Development and evaluation of an Earth-System model – HadGEM2, *Geosci. Model Dev.*, 4, 1051–1075, doi:10.5194/gmd-4-1051-2011, 2011.

Contoux, C., Ramstein, G., and Jost, A.: Modelling the mid-Pliocene Warm Period climate with the IPSL coupled model and its atmospheric component LMDZ5A, *Geosci. Model Dev.*, 5, 903–917, doi:10.5194/gmd-5-903-2012, 2012.

Tropical cyclone genesis

J. H. Koh and
C. M. Brierley

Title Page

Abstract

Introduction

Conclusions

References

Tables

Figures



Back

Close

Full Screen / Esc

Printer-friendly Version

Interactive Discussion



- DiNezio, P. N. and Tierney, J. E.: The effect of sea level on glacial Indo-Pacific climate, *Nat. Geosci.*, 6, 485–491, doi:10.1038/ngeo1823, 2013.
- DiNezio, P. N., Clement, A. C., Vecchi, G. A., Soden, B. J., Broccoli, A. J., Ottobliesner, B. L., and Braconnot, P.: The response of the Walker circulation to Last Glacial Maximum forcing: implications for detection in proxies, *Paleoceanography*, 26, PA3217, doi:10.1029/2010PA002083, 2011.
- Dowsett, H. J., Robinson, M. M., Stoll, D. K., and Foley, K. M.: Mid-Piacenzian mean annual sea surface temperature analysis for data-model comparisons, *Stratigraphy*, 7, 189–198, 2010.
- Dufresne, J. L., Foujols, M. A., Denvil, S., Caubel, A., Marti, O., Aumont, O., Balkanski, Y., Bekki, S., Bellenger, H., Benshila, R., Bony, S., Bopp, L., Braconnot, P., Brockmann, P., Cadule, P., Cheruy, F., Codron, F., Cozic, A., Cugnet, D., de Noblet, N., Duvel, J. P., Ethé, C., Fairhead, L., Fichefet, T., Flavoni, S., Friedlingstein, P., Grandpeix, J. Y., Guez, L., Guilyardi, E., Hauglustaine, D., Hourdin, F., Idelkadi, A., Ghattas, J., Jousssaume, S., Kageyama, M., Krinner, G., Labetoulle, S., Lahellec, A., Lefebvre, M. P., Lefevre, F., Levy, C., Li, Z. X., Lloyd, J., Lott, F., Madec, G., Mancip, M., Marchand, M., Masson, S., Meurdesoif, Y., Mignot, J., Musat, I., Parouty, S., Polcher, J., Rio, C., Schulz, M., Swingedouw, D., Szopa, S., Talandier, C., Terray, P., Viovy, N., and Vuichard, N.: Climate change projections using the IPSL-CM5 Earth System Model: from CMIP3 to CMIP5, *Clim. Dynam.*, 40, 2123–2165, 2013.
- Emanuel, K. A.: The maximum intensity of hurricanes, *J. Atmos. Sci.*, 45, 1143–1155, 1988.
- Emanuel, K. A.: The theory of hurricanes, *Annu. Rev. Fluid Mech.*, 23, 179–196, 1991.
- Emanuel, K. A.: *Atmospheric Convection*, Oxford University Press, Oxford, U. K., 1994.
- Emanuel, K. A.: Potential intensity algorithm, available at: <ftp://texmex.mit.edu/pub/emanuel/TCMAX/>, last accessed: 15 April 2014, 1998.
- Emanuel, K. A.: Sensitivity of tropical cyclones to surface exchange coefficients and a revised steady-state model incorporating eye dynamics, *J. Atmos. Sci.*, 52, 3969–3976, 1995a.
- Emanuel, K. A.: The behavior of a simple hurricane model using a convective scheme based on subcloud-layer entropy equilibrium, *J. Atmos. Sci.*, 52, 3960–3968, 1995b.
- Emanuel, K. A.: Tropical cyclones, *Annu. Rev. Earth Pl. Sc.*, 31, 75–104, 2003.
- Emanuel, K. A.: Downscaling CMIP5 climate models shows increased tropical cyclone activity over the 21st century, *P. Natl. Acad. Sci. USA*, 110, 12219–12224, 2013.
- Emanuel, K. A. and Nolan, D. S.: Tropical cyclone activity and the global climate system: In Preprints for 26th Conference on Hurricanes and Tropical Meteorology, Miami, Florida, Amer. Meteorol. Soc., Boston, 2004.

Tropical cyclone genesis

J. H. Koh and
C. M. Brierley

Title Page

Abstract

Introduction

Conclusions

References

Tables

Figures



Back

Close

Full Screen / Esc

Printer-friendly Version

Interactive Discussion



- Emanuel, K. A., Sundararajan, R., and Williams, J.: Hurricanes and global warming: results from downscaling IPCC AR4 simulations, *B. Am. Meteorol. Soc.*, 89, 347–367, 2008.
- Fedorov, A. V., Brierley, C. M., and Emanuel, K.: Tropical cyclones and permanent El Niño in the early Pliocene epoch, *Nature*, 463, 1066–1070, 2010.
- 5 Fedorov, A. V., Brierley, C. M., Lawrence, K. T., Liu, Z., Dekens, P. S., and Ravelo, A. C.: Patterns and mechanisms of early Pliocene warmth, *Nature*, 496, 43–49, 2013.
- Frank, W. M. and Ritchie, E. A.: Effects of vertical wind shear on the intensity and structure of numerically simulated hurricanes, *Mon. Weather Rev.*, 129, 2249–2269, 2001.
- Gagan, M. K., Ayliffe, L. K., Hopley, D., Cali, J. A., Mortimer, G. E., Chappell, J., McCulloch, M. T., and Head, M. J.: Temperature and surface-ocean water balance of the mid-Holocene tropical western Pacific, *Science*, 279, 1014–1018, 1998.
- 10 Gent, P. R., Danabasoglu, G., Donner, L. J., Holland, M. M., Hunke, E. C., Jayne, S. R., Lawrence, D. M., Neale, R. B., Rasch, P. J., and Vertenstein, M.: The Community Climate System Model Version 4, *J. Climate*, 24, 4973–4991, 2011.
- 15 Gordon, C., Cooper, C., Senior, C. A., Banks, H., Gregory, J. M., Johns, T. C., Mitchell, J. F. B., and Wood, R. A.: The simulation of SST, sea ice extents and ocean heat transports in a version of the Hadley Centre coupled model without flux adjustments, *Clim. Dynam.*, 16, 147–168, 2000.
- Gray, W. M.: Global view of the origin of tropical disturbances and storms, *Mon. Weather Rev.*, 96, 669–700, 1968.
- 20 Gray, W. M.: *Tropical Cyclone Genesis in the Western North Pacific*, Colorado State University, Fort Collins, Colorado, 1975.
- Haywood, A. M., Dowsett, H. J., Valdes, P. J., Lunt, D. J., Francis, J. E., and Sellwood, B. W.: Introduction. Pliocene climate, processes and problems, *Philos. T. R. Soc. A*, 367, 3–17, 2009.
- 25 Haywood, A. M., Dowsett, H. J., Robinson, M. M., Stoll, D. K., Dolan, A. M., Lunt, D. J., Otto-Bliesner, B., and Chandler, M. A.: Pliocene Model Intercomparison Project (PlioMIP): experimental design and boundary conditions (Experiment 2), *Geosci. Model Dev.*, 4, 571–577, doi:10.5194/gmd-4-571-2011, 2011.
- 30 Holland, G. J.: The maximum potential intensity of tropical cyclones, *J. Atmos. Sci.*, 54, 2519–2541, 1997.
- Jansen, E., Overpeck, J., Briffa, K. R., Duplessy, J.-C., Joos, F., Masson-Delmotte, V., Olago, D., Otto-Bliesner, B., Peltier, W. R., Rahmstorf, S., Ramesh, R., Raynaud, D., Rind, D., Solom-

Tropical cyclone genesis

J. H. Koh and
C. M. Brierley

Title Page

Abstract

Introduction

Conclusions

References

Tables

Figures



Back

Close

Full Screen / Esc

Printer-friendly Version

Interactive Discussion



ina, O., Villalba, R., and Zhang, D.: Paleoclimate, in: *Climate Change 2007: The Physical Science Basis. Contribution of Working Group I to the Fourth Assessment Report of the Intergovernmental Panel on Climate Change*, edited by: Solomon, S. et al., Cambridge University Press, New York City, 433–498, 2007.

5 Jourdain, N. C., Marchesiello, P., Menkes, C. E., Lefèvre, J., Vincent, E. M., Lengaigne, M., and Chauvin, F.: Mesoscale simulation of tropical cyclones in the South Pacific: climatology and interannual variability, *J. Climate*, 24, 3–25, 2010.

Kamae, Y., Ueda, H., and Kitoh, A.: Hadley and Walker circulations in the mid-Pliocene warm period simulated by an atmospheric general circulation model, *J. Meteorol. Soc. Jpn.*, 89, 10 475–493, 2011.

Klotzbach, P. J.: Trends in global tropical cyclone activity over the past twenty years (1986–2005), *Geophys. Res. Lett.*, 33, L10805, doi:10.1029/2006GL025881, 2006.

Knapp, K. R., Kruk, M. C., Levinson, D. H., Diamond, H. J., and Neumann, C. J.: The International Best Track Archive for Climate Stewardship (IBTrACS), *B. Am. Meteorol. Soc.*, 91, 15 363–376, doi:10.1175/2009BAMS2755.1, 2010.

Knutson, T. R., McBride, J. L., Chan, J., K. Emanuel, Holland, G., Landsea, C., Held, I., Kossin, J. P., Srivastava, A. K., and Sugi, M.: Tropical cyclones and climate change, *Nat. Geosci.*, 3, 157–163, 2010.

20 Knutson, T. R., Sirutis, J. J., Vecchi, G. A., Garner, S., Zhao, M., Kim, H.-S., Bender, M., Tuleya, R. E., Held, I. M and Villarini, G.: Dynamical downscaling projections of twenty-first-century Atlantic hurricane activity: CMIP3 and CMIP5 model-based scenarios, 26, 6591–6617, doi:10.1175/JCLI-D-12-00539.1, 2013.

Korty, R. L., Camargo, S. J., and Galewsky, J.: Tropical cyclone genesis factors in simulations of the Last Glacial Maximum, *J. Climate*, 25, 4348–4365, 2012a.

25 Korty, R. L., Camargo, S. J., and Galewsky, J.: Variations in tropical cyclone genesis factors in simulations of the Holocene epoch, *J. Climate*, 25, 8196–8211, 2012b.

Kossin, J. P., Emanuel, K. A., and Vecchi, G. A.: The poleward migration of the location of tropical cyclone maximum intensity, *Nature*, 509, 349–352, 2014.

Koutavas, A., Lynch-Stieglitz, J., Marchitto, T. M., and Sachs, J. P.: El Niño-like pattern in ice age tropical Pacific sea surface temperature, *Science*, 297, 226–230, 2002.

30 Kuhnert, H., Kuhlmann, H., Mohtadi, M., Meggers, H., Baumann, K.-H., and Pätzold, J.: Holocene tropical Western Indian Ocean sea surface temperatures in covari-

Tropical cyclone genesis

J. H. Koh and
C. M. Brierley

Title Page

Abstract

Introduction

Conclusions

References

Tables

Figures



Back

Close

Full Screen / Esc

Printer-friendly Version

Interactive Discussion



ation with climatic changes in the Indonesian region, *Paleoceanography*, 29, 423–437, doi:10.1002/2013PA002555 2014.

Lewis, S. and Maslin, M.: Defining humans as a geological power, *Nature*, in press, 2015.

Li, L., Lin, P., Yu, Y., Wang, B., Zhou, T., Liu, L., Liu, J., Bao, Q., Xu, S., Huang, W., Xia, K., Pu, Y., Dong, L., Shen, S., Liu, Y., Hu, N., Liu, M., Sun, W., Shi, X., Zheng, W., Wu, B., Song, M., Liu, H., Zhang, X., Wu, G., Xue, W., Huang, X., Yang, G., Song, Z., and Qiao, F.: The flexible global ocean–atmosphere–land system model, grid-point version 2: FGOALS-g2, *Adv. Atmos. Sci.*, 30, 543–560, 2013.

Luan, Y., Braconnot, P., Yu, Y., Zheng, W., and Marti, O.: Early and mid-Holocene climate in the tropical Pacific: seasonal cycle and interannual variability induced by insolation changes, *Clim. Past*, 8, 1093–1108, doi:10.5194/cp-8-1093-2012, 2012.

Lucas, C., Timbal, B., and Nguyen, H.: The expanding tropics: a critical assessment of the observational and modeling studies, *Climate Change*, 5, 89–112, 2014.

Menkes, C. E., Lengaigne, M., Marchesiello, P., Jourdain, N. C., Vincent, E. M., Lefèvre, J., Chauvin, F., and Royer, J.-F.: Comparison of tropical cyclogenesis indices on seasonal to interannual timescales, *Clim. Dynam.*, 38, 301–321, 2012.

Montgomery, M. T., Smith, R. K., and Nguyen, S. V.: Sensitivity of tropical-cyclone models to the surface drag coefficient, *Q. J. Roy. Meteor. Soc.*, 136, 1945–1953, 2010.

Nolan, D. S. and Rappin, E. D.: Increased sensitivity of tropical cyclogenesis to wind shear in higher SST environments, *Geophys. Res. Lett.*, 35, L14805, doi:10.1029/2008GL034147, 2008.

Pagani, M., Z. Liu, LaRiviere, J., and Ravelo, A. C.: High Earth-system climate sensitivity determined from Pliocene carbon dioxide concentrations, *Nat. Geosci.*, 3, 27–30, 2009.

Riemer, M., Montgomery, M. T., and Nicholls, M. E.: Further examination of the thermodynamic modification of the inflow layer of tropical cyclones by vertical wind shear, *Atmos. Chem. Phys.*, 13, 327–346, doi:10.5194/acp-13-327-2013, 2013.

Rimbu, N., Lohmann, G., Lorenz, S. J., Kim, J. H., and Schneider, R. R.: Holocene climate variability as derived from alkenone sea surface temperature and coupled ocean–atmosphere model experiments, *Clim. Dynam.*, 23, 215–227, 2004.

Robinson, M. M., Dowsett, H. J., and Chandler, M. A.: Pliocene role in assessing future climate impacts, *Eos T. Am. Geophys. Un.*, 89, 501–502, 2008.

Tropical cyclone genesis

J. H. Koh and
C. M. Brierley

[Title Page](#)

[Abstract](#)

[Introduction](#)

[Conclusions](#)

[References](#)

[Tables](#)

[Figures](#)



[Back](#)

[Close](#)

[Full Screen / Esc](#)

[Printer-friendly Version](#)

[Interactive Discussion](#)



Stott, L., K. Cannariato, Thunell, R., Haug, G. H., Koutavas, A., and Lund, S.: Decline of surface temperature and salinity in the western tropical Pacific Ocean in the Holocene epoch, *Nature*, 431, 56–59, 2004.

Sueyoshi, T., Ohgaito, R., Yamamoto, A., Chikamoto, M. O., Hajima, T., Okajima, H., Yoshimori, M., Abe, M., O'ishi, R., Saito, F., Watanabe, S., Kawamiya, M., and Abe-Ouchi, A.: Set-up of the PMIP3 paleoclimate experiments conducted using an Earth system model, MIROC-ESM, *Geosci. Model Dev.*, 6, 819–836, doi:10.5194/gmd-6-819-2013, 2013.

Tippett, M. K., Camargo, S. J., and Sobel, A. H.: A Poisson regression index for tropical cyclone genesis and the role of large-scale vorticity in genesis, *J. Climate*, 24, 2335–2357, 2010.

Tory, K. J., Dare, R. A., Davidson, N. E., McBride, J. L., and Chand, S. S.: The importance of low-deformation vorticity in tropical cyclone formation, *Atmos. Chem. Phys.*, 13, 2115–2132, doi:10.5194/acp-13-2115-2013, 2013.

Vecchi, G. A., Swanson, K. L., and Soden, B. J.: Whither hurricane activity, *Science*, 322, 687–689, doi:10.1126/science.1164396, 2008.

Velden, C. S. and Sears, J.: Computing deep-tropospheric vertical wind shear analyses for tropical cyclone applications: does the methodology matter?, *Weather Forecast.*, 29, 1169–1180. doi:10.1175/WAF-D-13-00147.1, 2014.

Waelbroeck, C., Paul, A., Kucera, M., Rosell-Melé, A., Weinelt, M., Schneider, R., Mix, A. C., Abelmann, A., Armand, L., Bard, E., Barker, S., Barrows, T. T., Benway, H., Cacho, I., Chen, M.-T., Cortijo, E., Crosta, X., de Vernal, A., Dokken, T., Duprat, J., Elderfield, H., Eynaud, F., Gersonde, R., Hayes, A., Henry, M., Hillaire-Marcel, C., Huang, C.-C., Jansen, E., Juggins, S., Kallel, N., Kiefer, T., Kienast, M., Labeyrie, L., Leclaire, H., Londeix, L., Mangin, S., Matthiessen, J., Marret, F., Meland, M., Morey, A. E., Mulitza, S., Pflaumann, U., Pisias, N. G., Radi, T., Rochon, A., Rohling, E. J., Sbaffi, L., Schaf er-Neth, C., Solignac, S., Spero, H., Tachikawa, K., and Turon, J.-L.: Constraints on the magnitude and patterns of ocean cooling at the Last Glacial Maximum, *Nat. Geosci.*, 2, 127–132, doi:10.1038/ngeo411, 2009.

Webster, P. J., Holland, G. J., Curry, J. A., and Chang, H. R.: Changes in tropical cyclone number, duration, and intensity in a warming environment, *Science*, 309, 1844–1846, 2005.

Tropical cyclone genesis

J. H. Koh and
C. M. Brierley

[Title Page](#)

[Abstract](#)

[Introduction](#)

[Conclusions](#)

[References](#)

[Tables](#)

[Figures](#)



[Back](#)

[Close](#)

[Full Screen / Esc](#)

[Printer-friendly Version](#)

[Interactive Discussion](#)



Table 2. List of GCMs used in this study along with their storm frequency and variability seen in the pre-industrial simulation.

Model	Atmospheric Resolution ° Lat × ° Lon × Levels	Storms per year	SD (%)	Reference
CCSM4	0.9 × 1.25 × 26	94	1.7	Gent et al. (2011)
FGOALS-G2	2.8 × 2.8 × 26	62	1.1	Li et al. (2013)
HADCM3	2.5 × 3.75 × 19	90	2.9	Gordon et al. (2000)
HADGEM2-ES (only RCP8.5)	1.25 × 1.875 × 38	43	–	Collins et al. (2011)
IPSL-CM5A	3.75 × 1.875 × 39	31	1.6	Dufresne et al. (2013)
MIROC-ESM	2.8 × 2.8 × 80	43	2.5	Sueyoshi et al. (2013)
MIROC4m (only Pliocene)	2.8 × 2.8 × 20	94	–	Chan et al. (2011)

Tropical cyclone genesis

J. H. Koh and
C. M. Brierley

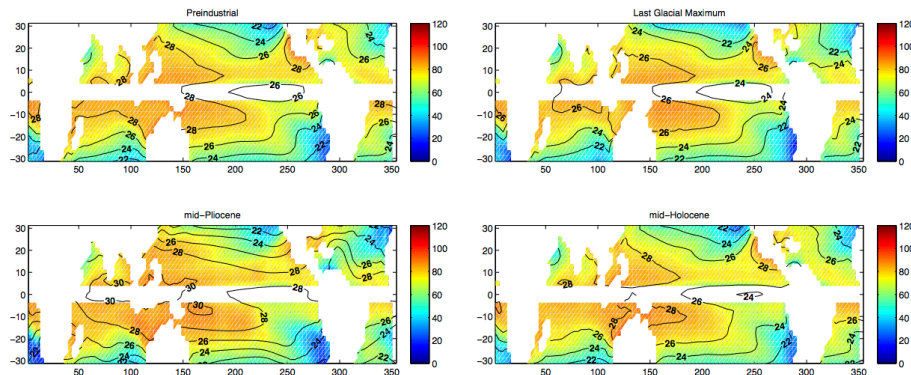


Figure 1. Sea surface temperature (contour lines) and potential intensity in Northern Hemisphere (NH) during July–October (JASO) and Southern Hemisphere (SH) during January–April (JFMA) for **(a)** pre-industrial control, **(b)** Pliocene, **(c)** LGM and **(d)** mid-Holocene. Units are SST ($^{\circ}\text{C}$) and potential intensity (m s^{-1}).

Title Page

Abstract

Introduction

Conclusions

References

Tables

Figures



Back

Close

Full Screen / Esc

Printer-friendly Version

Interactive Discussion



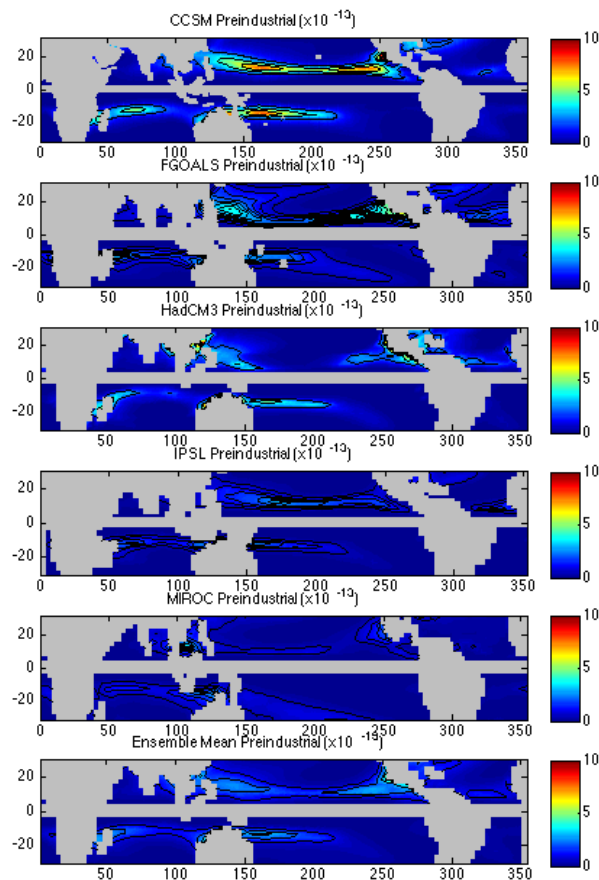
Tropical cyclone
genesisJ. H. Koh and
C. M. Brierley

Figure 2. Pre-industrial control GPI from (a) CCSM4, (b) FGOALS-G2, (c) HadCM3, (d) IPSL-CM5A-LR, (e) MIROC-ESM and (f) ensemble. Northern Hemisphere depicts JASO monthly mean GPI while Southern Hemisphere depicts JFMA monthly mean GPI. Units are occurrences $\text{m}^{-2} \text{month}^{-1}$.

Title Page

Abstract

Introduction

Conclusions

References

Tables

Figures



Back

Close

Full Screen / Esc

Printer-friendly Version

Interactive Discussion



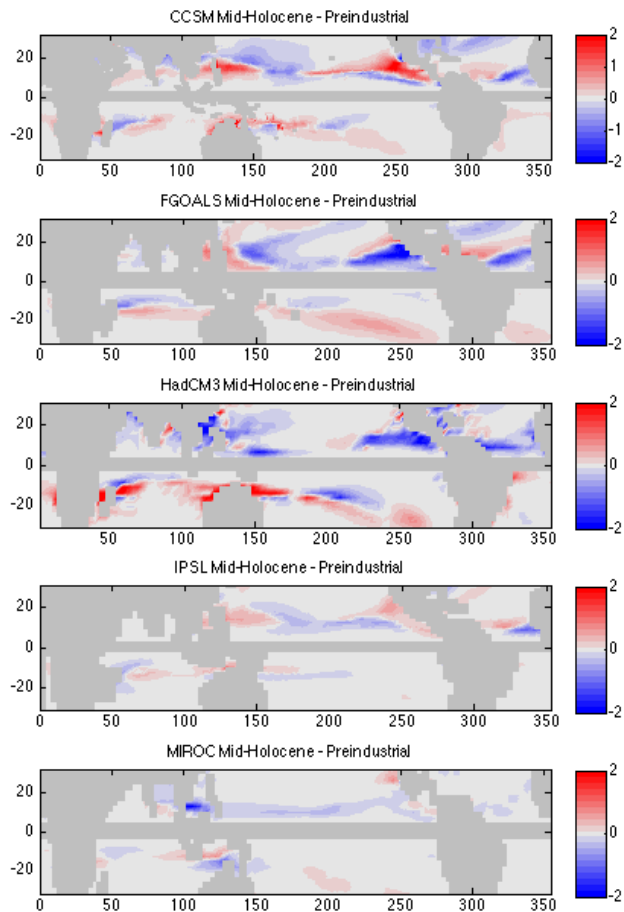


Figure 3. Cyclone genesis difference between mid-Holocene and PI in Northern Hemisphere (JASO) and Southern Hemisphere (JFMA) for **(a)** CCSM4, **(b)** FGOALS, **(c)** HadCM3, **(d)** IPSL, **(e)** MIROC. Units are occurrences $m^{-2} month^{-1}$.

**Tropical cyclone
genesis**

J. H. Koh and
C. M. Brierley

Title Page

Abstract

Introduction

Conclusions

References

Tables

Figures

◀

▶

◀

▶

Back

Close

Full Screen / Esc

Printer-friendly Version

Interactive Discussion



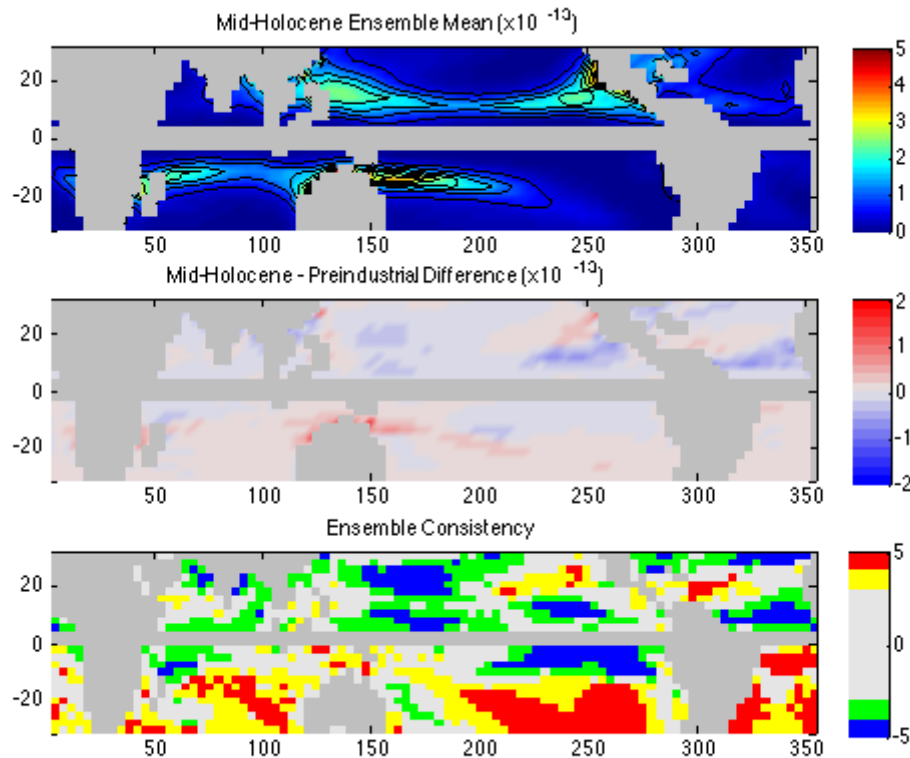


Figure 4. (a) Mid-Holocene ensemble GPI, (b) mid-Holocene and pre-industrial control ensemble GPI difference, and (c) robustness of the palaeoclimate genesis signals, as indicated by the number of models agreeing with the direction of the change. Yellow and red denote areas for model agreement on positive sign change. Green and blue areas denote model agreement on negative sign change. Northern Hemisphere depicts JASO season, while Southern Hemisphere depicts JFMA season. Units in (a) and (b) are occurrences $\text{m}^{-2} \text{month}^{-1}$.

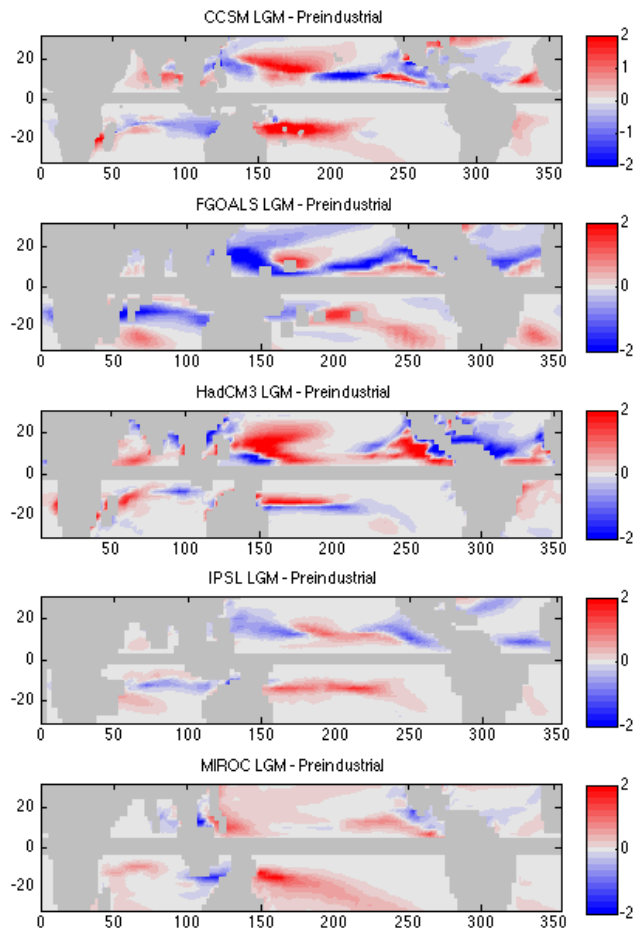


Figure 5. Cyclone genesis difference between LGM and PI in Northern Hemisphere (JASO) and Southern Hemisphere (JFMA) for (a) CCSM4, (b) FGOALS, (c) HadCM3, (d) IPSL, (e) MIROC. Units are occurrences $\text{m}^{-2} \text{month}^{-1}$.

**Tropical cyclone
genesis**

J. H. Koh and
C. M. Brierley

Title Page

Abstract Introduction

Conclusions References

Tables Figures

◀ ▶

◀ ▶

Back Close

Full Screen / Esc

Printer-friendly Version

Interactive Discussion



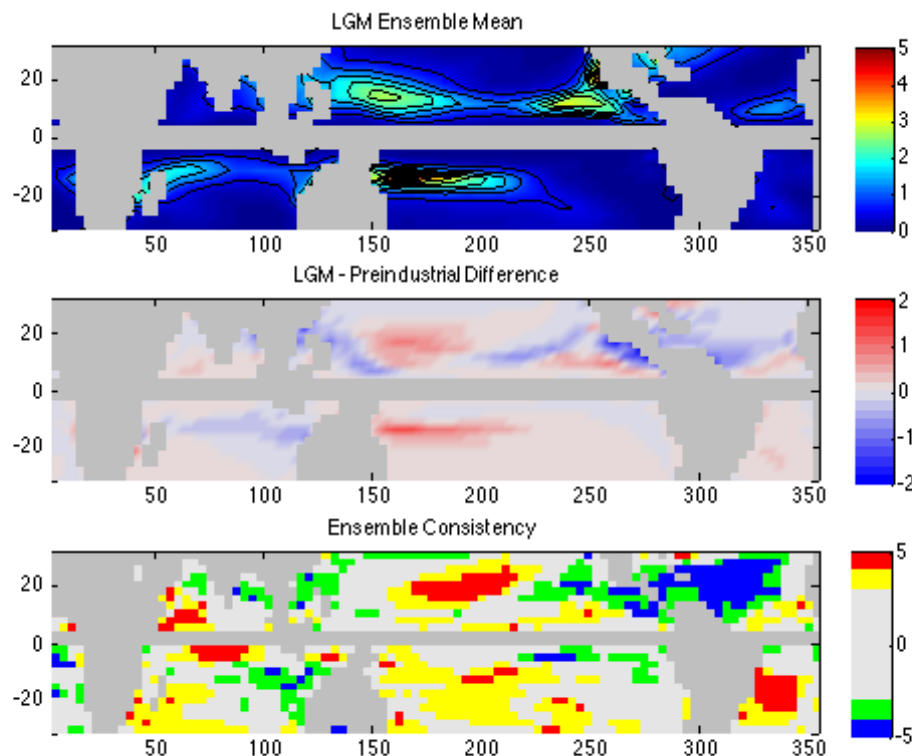
Tropical cyclone
genesisJ. H. Koh and
C. M. Brierley

Figure 6. (a) LGM ensemble GPI (b) LGM and pre-industrial control ensemble GPI difference, and (c) robustness of the palaeoclimate genesis signals, as indicated by the number of models agreeing with the direction of the change. Yellow and red denote areas for model agreement on positive sign change. Green and blue areas denote model agreement on negative sign change. White areas denote regions where less than four models agree. Northern Hemisphere depicts JASO season, while Southern Hemisphere depicts JFMA season. Units in (a) and (b) are occurrences $10^{13} \text{ m}^{-2} \text{ month}^{-1}$.

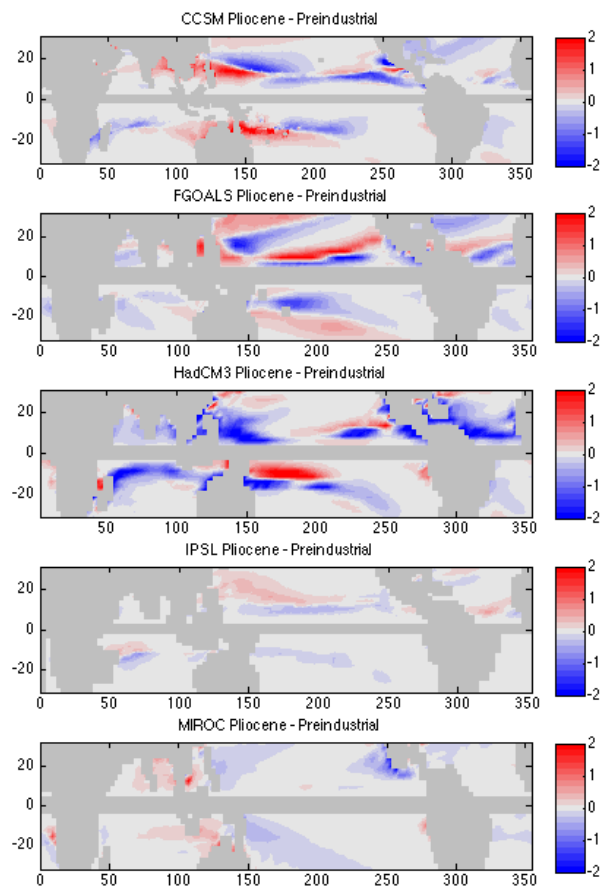
**Tropical cyclone
genesis**J. H. Koh and
C. M. Brierley

Figure 7. Cyclone genesis difference between Pliocene and PI in Northern Hemisphere (JASO) and Southern Hemisphere (JFMA) for (a) CCSM4, (b) FGOALS, (c) HadCM3, (d) IPSL, (e) MIROC.

[Title Page](#)[Abstract](#)[Introduction](#)[Conclusions](#)[References](#)[Tables](#)[Figures](#)[Back](#)[Close](#)[Full Screen / Esc](#)[Printer-friendly Version](#)[Interactive Discussion](#)

Tropical cyclone
genesisJ. H. Koh and
C. M. Brierley

Title Page

Abstract

Introduction

Conclusions

References

Tables

Figures



Back

Close

Full Screen / Esc

Printer-friendly Version

Interactive Discussion

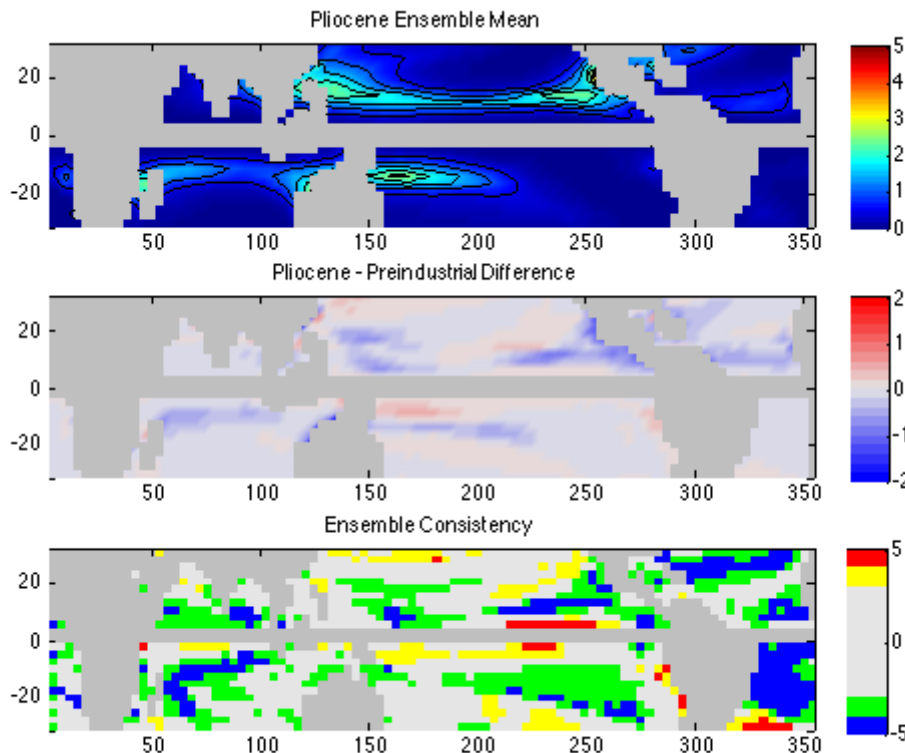


Figure 8. (a) Pliocene ensemble GPI (b) Pliocene and pre-industrial control ensemble GPI difference, and (c) robustness of the palaeoclimate genesis signals, as indicated by the number of models agreeing with the direction of the change. Yellow and red denote areas for model agreement on positive sign change. Green and blue areas denote model agreement on negative sign change. White areas denote regions where less than four models agree. Northern Hemisphere depicts JASO season while Southern Hemisphere depicts JFMA season. Units in (a) and (b) are occurrences $10^{13} \text{ m}^{-2} \text{ month}^{-1}$.

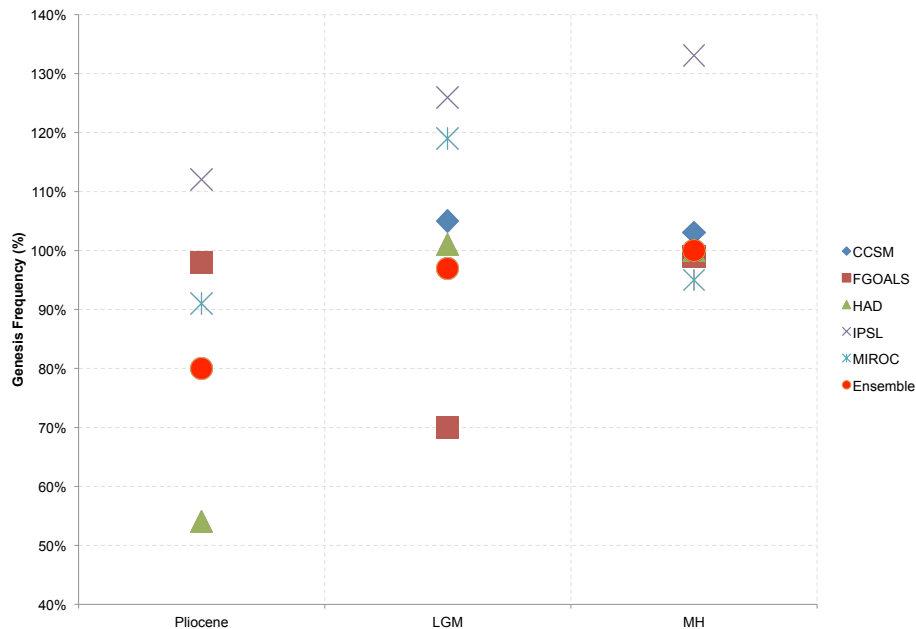
**Tropical cyclone
genesis**J. H. Koh and
C. M. Brierley

Figure 9. Model and ensemble annual cyclone genesis frequency as percentage of pre-industrial control frequency.

[Title Page](#)[Abstract](#)[Introduction](#)[Conclusions](#)[References](#)[Tables](#)[Figures](#)[Back](#)[Close](#)[Full Screen / Esc](#)[Printer-friendly Version](#)[Interactive Discussion](#)

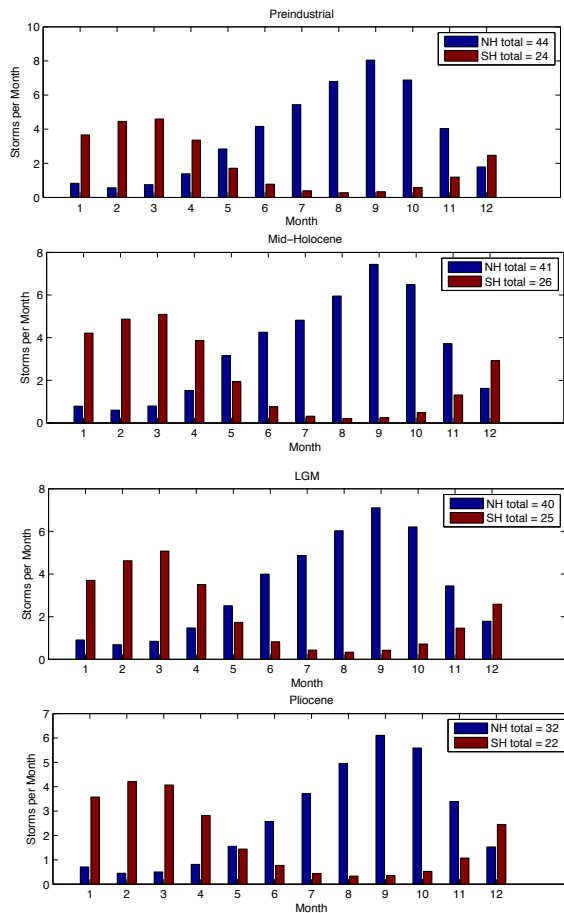
Tropical cyclone
genesisJ. H. Koh and
C. M. Brierley

Figure 10. Northern Hemisphere (NH) and Southern Hemisphere (SH) ensemble monthly and annual cyclone genesis frequency for (a) Pliocene (b) LGM, (c) mid-Holocene and (d) pre-industrial control.

Tropical cyclone genesis

J. H. Koh and
C. M. Brierley

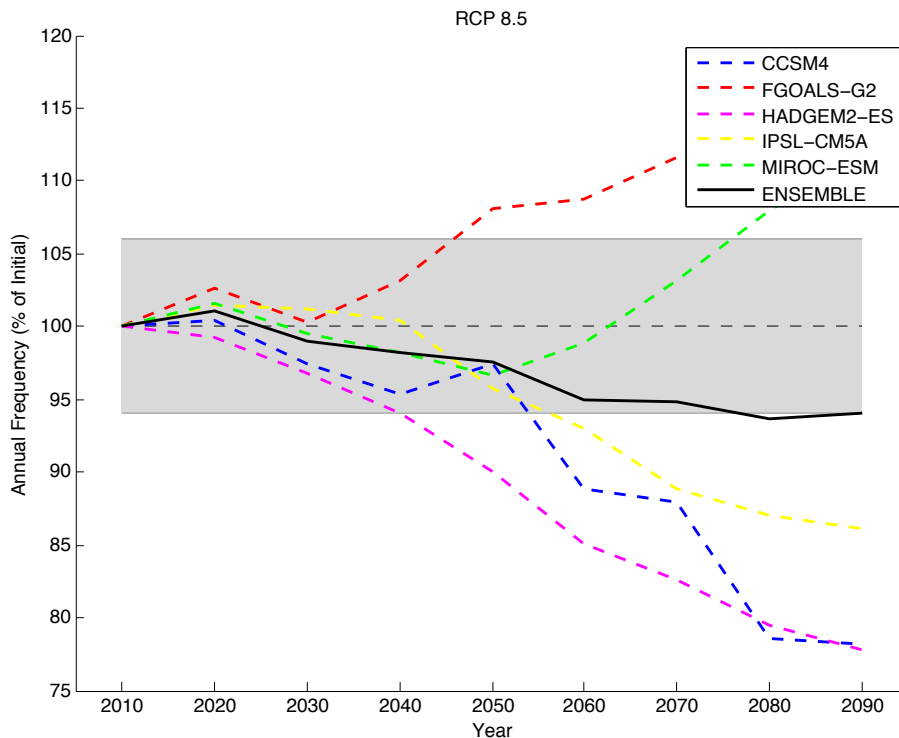


Figure 11. RCP8.5 annual cyclone genesis frequency projection between 2005–2095. The shaded area represents the spread expected from internal variability alone, from the baseline of 80 occurrences observed in modern day (black dashed line).

[Title Page](#)

[Abstract](#) | [Introduction](#)

[Conclusions](#) | [References](#)

[Tables](#) | [Figures](#)

[◀](#) | [▶](#)

[◀](#) | [▶](#)

[Back](#) | [Close](#)

[Full Screen / Esc](#)

[Printer-friendly Version](#)

[Interactive Discussion](#)

